Multiple-histogram method for quantum Monte Carlo simulations

C. L. Martin*
Physics Department, University of California, Santa Barbara, California 93106
(Received 14 August 1998; revised manuscript received 16 October 1998)

An extension to the multiple-histogram method (sometimes referred to as the Ferrenberg-Swendsen method) for use in quantum Monte Carlo simulations is presented. This method is shown to work well for the two-dimensional repulsive Hubbard model, allowing measurements to be taken over a continuous region of parameters. The method also reduces the error bars over the range of parameter values due to the overlapping of multiple histograms. A continuous sweep of parameters and reduced error bars allow one to make more difficult measurements, such as Maxwell constructions used to study phase separation. Possibilities also exist for this method to be used for other quantum systems. [S0163-1829(99)09703-9]

I. INTRODUCTION

When making calculations using the Monte Carlo method, one often would like to make measurements of some observable as a function of the parameters of the Hamiltonian. To do this the standard procedure is to perform a run at one setting of the parameters until a measurement of the observable with sufficiently small error bars is produced. One then moves on to another setting of the parameters, and so on until a large discrete set of measurements of the observable is produced. This can require large amounts of computer time depending on the details of the Hamiltonian and the Monte Carlo method one has chosen. Building an approximation of a continuous function for the desired observable point by point would require an even larger set of discrete points, and a related increase in computer time.

Continuous functions of observables are useful for innumerable activities, such as verifying functional dependencies and looking for phase separation using Maxwell constructions.[1] The multiple-histogram method[2] (MHM) allows one to produce these continuous functions for a classical Hamiltonian. In this paper, it will be shown that under certain circumstances the MHM can also be applied to quantum-mechanical Hamiltonians as well, for example the two-dimensional Hubbard model.[3] Observables of this Hamiltonian will be measured using standard quantum Monte Carlo (QMC) techniques[4] and the MHM will be applied to obtain observables as continuous functions of the parameters of the system. As in the classical case, the use of overlapping histograms reduces the errors below those of a single measurement. Furthermore, the MHM will be applied specifically to the density and energy of the Hubbard model as functions of the chemical potential to search for signs of phase separation.

II. SINGLE HISTOGRAM METHOD

In order to obtain a variable as a continuous function of thermodynamic variables like the inverse temperature $\beta=(k_BT)^{-1}$ and the chemical potential μ, one can use a technique originally used by Salsburg *et al.*,[5] extended by Valleau and Card,[6] and further extended by Swendsen and Ferrenberg.[2,7] To see how this can be done for the chemical potential μ, let us assume we have a classical Hamiltonian,

$$\mathcal{H}=E-\mu N, \tag{1}$$

where E is the energy and N is the particle number. From this Hamiltonian, one can derive a partition function for a particular value of μ,

$$Z_\mu=\sum_n \rho(n)e^{\beta\mu n}, \tag{2}$$

where $\rho(n)$ is a density of states, which for these purposes we can leave undetermined, and n is the particle density. We can also derive a probability to have a given density for this value of μ,

$$P_\mu(n)=\frac{\rho(n)e^{\beta\mu n}}{Z_\mu}. \tag{3}$$

Substituting Eq. (2) into Eq. (3) allows us to find the probability for a value of n at an arbitrary value of the chemical potential μ',

$$P_{\mu'}(n)=\frac{P_\mu(n)e^{\beta(\mu'-\mu)n}}{\sum_n P_\mu(n)e^{\beta(\mu'-\mu)n}}. \tag{4}$$

III. MULTIPLE-HISTOGRAM METHOD

Equation (4) can be extended for use with many histograms taken at varying parameters, as discussed in detail by Ferrenberg and Swendsen in Ref. 2. Consider a situation where we have m runs of a simulation labeled by an index $i=\{1,\ldots,m\}$. We perform the ith simulation at a chemical potential μ_i, and store the results as an unnormalized histogram $N_i(n)$.

We follow the same general procedure as described above for the single-histogram method (for more details see Ref. 2) and acquire a function for the probability of a density n, at a chemical potential μ' based all on all m runs.

$$P_{\mu'}(n)=\frac{\sum_{i=1}^{m} g_i^{-1}N_i(n)\exp(\beta\mu' n)}{\sum_{j=1}^{m}\left[\sum_n N_j(n)\right]g_j^{-1}\exp(\beta\mu_j n-f_j)}, \quad (5)$$

where f_j is calculated self-consistently based on the definition

$$\exp(f_j)=\sum_n P_{\mu_j}(n), \quad (6)$$

and $g_j=1+2\tau_j$ is defined by the autocorrelation times τ_j of the successive measurements of n.

In order to avoid histograms at values of μ_i far removed from the value μ' being calculated from overwhelming the calculation, it was found to be necessary to introduce a Gaussian cutoff of the form,

$$\tilde{N}_i(n,\mu')=N_i(n)\exp[-\Lambda(\mu_i-\mu')^2]. \quad (7)$$

$\tilde{N}_i(n,\mu')$ is then used in place of $N_i(n)$ in Eq. (5), and Λ is set to a fixed value (depending on the spacing of μ_i's) that allows only the nearest four to six histograms to contribute to a calculation for a given μ'.

Using multiple histograms in this manner allows one to increase the range of validity of the technique, and reduce the resulting error bars over the entire range of parameters.

IV. MHM WITH THE HUBBARD MODEL

To demonstrate the use of this method for quantum Hamiltonians, the Hubbard Hamiltonian[3] will be used

$$H=-t\sum_{\langle ij\rangle}\sum_{\sigma=\{\uparrow\downarrow\}}(\hat{c}_{i\sigma}^{\dagger}\hat{c}_{j\sigma}+\hat{c}_{j\sigma}^{\dagger}\hat{c}_{i\sigma}) +U\sum_i\left(\hat{n}_{i\uparrow}-\frac{1}{2}\right)\left(\hat{n}_{i\downarrow}-\frac{1}{2}\right)-\mu\sum_i(\hat{n}_{i\uparrow}+\hat{n}_{i\downarrow}), \quad (8)$$

where t is a parameter to set the strength of electron hopping (kinetic energy), $\hat{c}_{i\sigma}^{(\dagger)}$ is the annihilation (creation) operator for an electron at site i with spin $\sigma=\{\uparrow\downarrow\}$, U is a parameter to set the strength of on-site Coulomb repulsion, μ is the chemical potential, and $\hat{n}_{i\sigma}=\hat{c}_{i\sigma}^{\dagger}\hat{c}_{i\sigma}$. Clearly there are quantum operators in the Hubbard Hamiltonian, so the classical derivation given earlier for the probability as a function of μ will only hold if the system happens to be in states of definite particle number. In determinantal QMC, a Hubbard-Stratonovich (HS) transformation[8] leads to a bilinear fermion form for the interaction. One sums over all possible fermion states and then over the HS field. Thus, a given HS configuration comes from a trace over all particle numbers so that it is not guaranteed that a given HS configuration will have a definite particle number. It is this feature that distinguishes this problem from the classical statistical-mechanics problem. However, if one finds that the various HS configurations are indeed characterized by an integer-fermion occupation, then as we will discuss, one can proceed. Here, for the two-dimensional (2D) Hubbard model near half filling, the charge gap provides an energy barrier to noninteger filling. As can be seen in Fig. 1, when one runs simulations at a sufficiently low temperature, one observes peaks in the histogram corresponding to states with integer numbers of holes. If these states truly have a definite number of particles, the peaks should scale using the grand canonical distribution for runs at different values of μ. In Fig. 2, the peaks at half filling $(n=1)$ are fit against the grand canonical probability

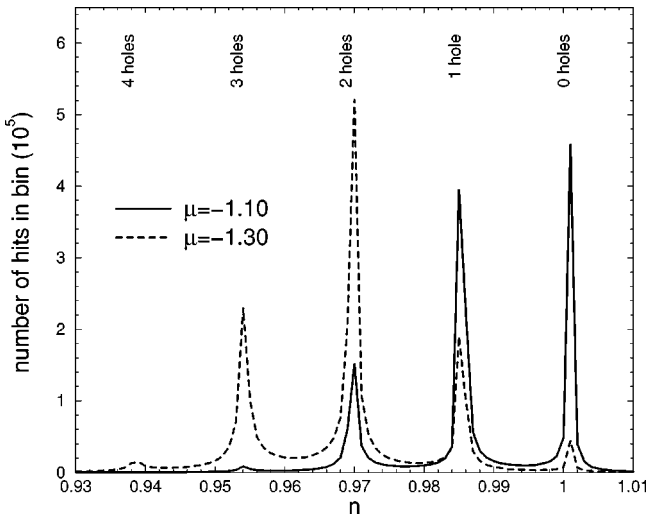

FIG. 1. A histogram of the particle density sampled after each sweep in a quantum Monte Carlo simulation of the Hubbard model on an 8 by 8 lattice with $\beta t=8$, $U/t=8$, and $\mu=-1.10$ and -1.30. One can see well-defined peaks at particle densities corresponding with integer numbers of holes. It is also possible to see how the two histograms at different parameters overlap each other, allowing one to be normalized with respect to the other.

$$P(N,\mu)=\frac{\exp[-\beta(E_N-\mu N)]}{\sum_N \exp[-\beta(E_N-\mu N)]}, \quad (9)$$

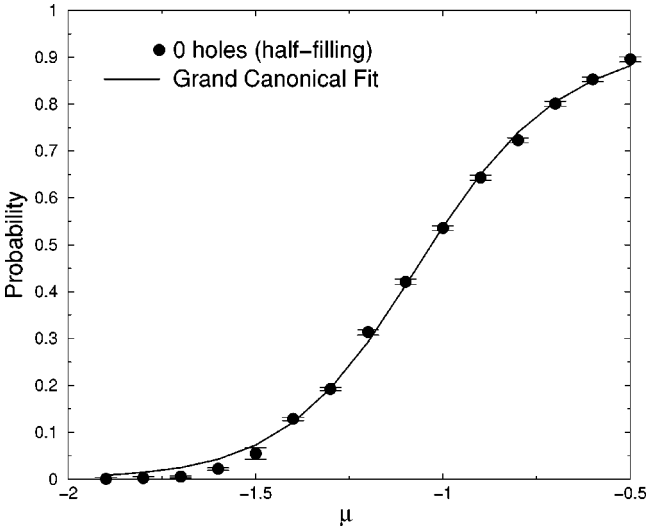

FIG. 2. Normalizing the peaks in histograms such as the ones shown in Fig. 1, yield the probability for a certain particle density. One can then change the μ used in the simulation and follow the relative probability of this peak as a function of μ. If the states truly have a definite particle density they should follow a curve given by the grand canonical distribution, which is shown in the solid line.

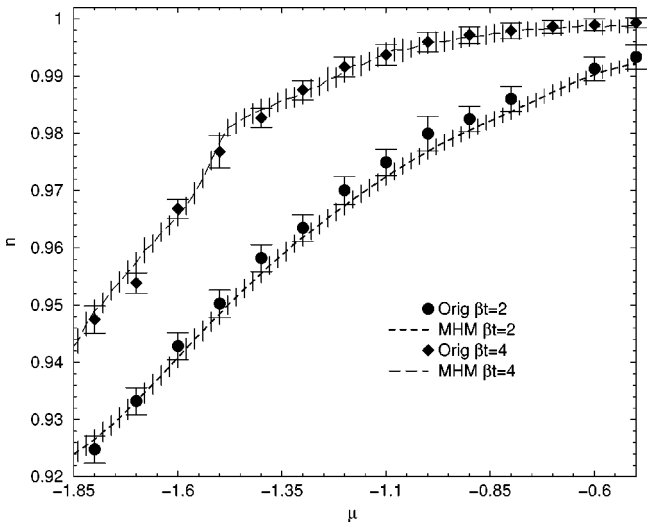

FIG. 3. The original points and the MHM method continuous curves are shown for the particle density (n) vs chemical potential (μ) for two values of the inverse temperature β. All simulations are performed on an 8 by 8 square lattice at $U/t=8$. Error bars on the original data points are shown as bars with hats originating from the points, and error bars on the MHM line are shown as bars without hats originating at regular intervals from the dashed line.

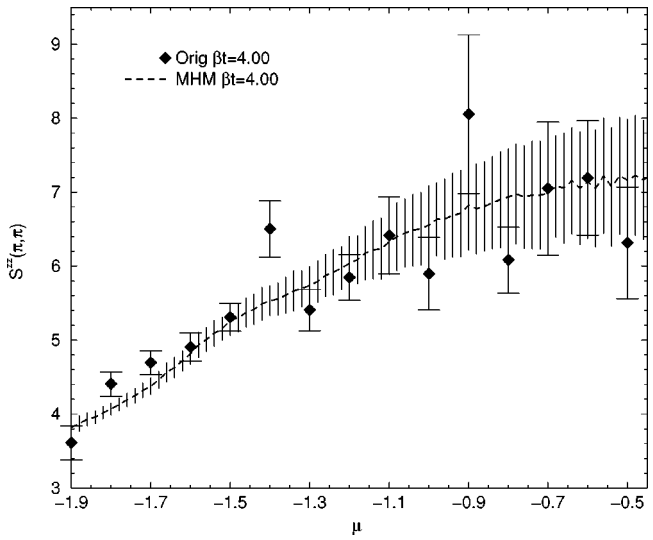

FIG. 4. Original points and the resulting MHM method continuous curve are shown for the equal time zz antiferromagnetic spin-correlation function $[S^{zz}(\pi,\pi)]$. As the parameters are moved closer to half filling ($\mu=0$), the system begins to develop antiferromagnetic order as shown by the increasing value of $S^{zz}(\pi,\pi)$. The simulations are performed on an 8 by 8 square lattice at $U/t=8$. Error bars on the original data points are shown as bars with hats originating from the points, and error bars on the MHM line are shown as bars without hats originating at regular intervals from the dashed line.

where E_N is the average measured energy for the states with particle number N.

Note that in Fig. 1, multiple histograms are presented in order to emphasize the fact that the MHM allows one to obtain even more information when several histograms are used. By normalizing each histogram with respect to the others, a continuous function of the desired observable may be obtained. In the results that follow, we have used many overlapping histograms in order to fully cover the range of simulation variables of interest.

In parameter regimes[9] where these peaks are present in the histograms of particle number, one can proceed to take any operator that conserves particle density and determine its behavior as a continuous function of μ. This can be done by using a reduced number of simulations at different values of μ, as long as the respective histograms of particle density overlap. To prevent unwanted overlap from very distant histograms, it was found necessary to introduce a Gaussian cutoff. The cutoff reduces the effective weight of a histogram as the difference between the value of μ for that histogram and the value of μ' at which the MHM method is run increases. As an added benefit, the error bars for this continuous function of μ will be reduced from those obtained from any one simulation, because one can use information about the operator from all of the simulations performed.

V. RESULTS

In Fig. 3 one can see what happens when the MHM is applied to a set of histograms measuring the particle number during a QMC simulation of the Hubbard model. The chemical potential μ is varied over a range starting from half filling ($\mu=0$ and, thus, $n=\langle\hat{n}\rangle=1$) through increasingly negative values of μ. The individual runs are shown as points with associated error bars, and the MHM is applied to get a continuous function of n vs μ with error bars shown as vertical bars around the dashed line. The error bars are checked through both the bootstrap method[10] and by incorporating the errors due to correlations in the reweighted samples and their finite size.[11] To see how the line changes with different values of the inverse temperature β, the process is repeated at $\beta t=4$.

As one can see, the error bars on the MHM line are comparable to those from the original points, and the MHM continuously fits the original points. As the simulation temperature decreases (large β) the sign problem[12] becomes much more severe. For the histogram method this means that while there are peaks in the histograms for n vs μ for configurations with positive signs, they are wiped out by nearly identical peaks with negative signs.

In Fig. 4, the MHM is applied to another interesting observable, the equal-time antiferromagnetic spin-correlation function $S^{zz}(\pi,\pi)$, the Fourier transform of $\langle(n_{i\uparrow}-n_{i\downarrow})(n_{j\uparrow}-n_{j\downarrow})\rangle$ taken at momentum (π,π). As the system moves closer to half filling ($\mu=0$), the antiferromagnetic order increases as expected.[13]

VI. PHASE SEPARATION

Recently, computational evidence for the existence of phase separation in the strongly correlated t-J and Hubbard models, both for and against, have been presented in the literature.[14] One of the best ways to search for phase separation is through the use of a Maxwell construction.[1] A Maxwell construction consists in its simplest form as a graph of free energy vs density. As we let the temperature become small, we can ignore the entropy term and just consider the

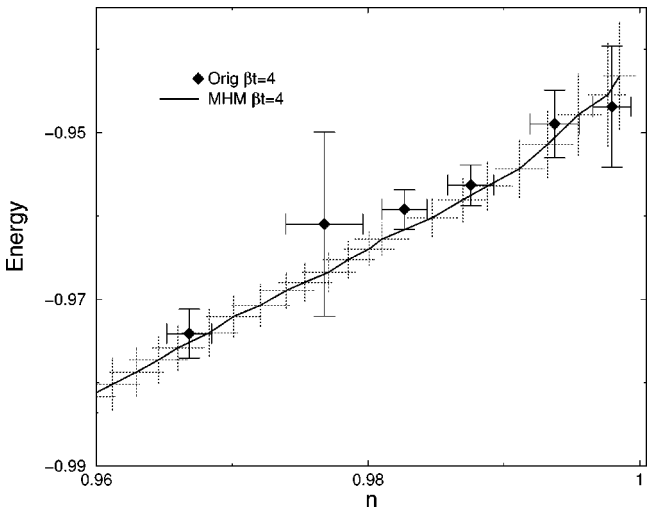

FIG. 5. Original points and the resulting MHM method continuous curve are shown for a Maxwell construction of energy vs particle density (n); some points have been omitted for clarity. Phase separation would be indicated by a region of the curve with upwards curvature, which appears in neither curve. Error bars for both the uncertainty in energy and particle density on the original data points are shown as bars with hats originating from the points, and error bars on the MHM line are shown as dotted bars without hats originating from the dashed line.

energy. Thermodynamics wants a system to minimize its free energy, and so a phase-separated region will appear on the graph as a region of upwards curvature ($\partial^2 E/\partial n^2 < 0$). In such a region the energy of the phase-separated state will be lower than that of the homogeneous state, and phase separation is thus favored. It is of interest, therefore, to apply the MHM to obtain continuous energy vs density measurements in order to investigate the possible existence of phase separation. In Fig. 5, a Maxwell construction for the 2D Hubbard model at $\beta t = 4$ is shown. With just the original data points it is nearly impossible to say anything definitive about the curvature of the line, however, when the MHM method is employed, the lack of any clear signs of upwards curvature becomes much more apparent. Thus, it is possible to conclude that one does not see phase separation for this range of parameters, a conclusion that would have been difficult to make without using the full information from the histograms. As further simulations are run at lower temperatures, it will be interesting to see if phase separation develops. It is expected that the MHM will allow us to improve the quality of the measurements, so that the simulations at these lower temperatures will be possible.

VII. CONCLUSIONS

In some circumstances, the MHM method can be used effectively for Hamiltonians containing quantum operators, such as the Hubbard Hamiltonian just described. The ability to generate continuous functions of an observable makes a number of analysis techniques much more feasible. For example, in order to perform a Maxwell construction,[1] a continuous function of energy as a function of particle density is desired. Previously, a function like this would have been constructed laboriously one point at a time using the averages of large simulations, and conclusions drawn using reasonable guesses about what function would fit the calculated points. Using the multiple-histogram method, the large quantity of information present in the histograms of each simulation is brought to bear using simple statistical physics arguments. The information from the simulations is thus used more efficiently and smaller error bars and reasonable continuous functions are produced.

ACKNOWLEDGMENTS

Support was received from the U.S. Department of Energy under Grant No. DE-FG03-85ER45197, and computer time on the Cray T90 at SDSC was provided by NPACI. Useful discussions and insights were generously provided by D. Scalapino, R. Sugar, D. Duffy, and E. Kim.

*Electronic address: chris@physics.ucsb.edu

[1] K. Huang, *Statistical Mechanics*, 2nd ed. (Wiley, New York, 1987), pp. 41-43 and 163-167.

[2] A. Ferrenberg and R. Swendsen, Phys. Rev. Lett. **63**, 1195 (1989).

[3] J. Hubbard, Proc. R. Soc. London, Ser. A **276**, 238 (1963).

[4] R. Blankenbecler, D. Scalapino, and R. Sugar, Phys. Rev. D **24**, 2278 (1981); J. Hirsch, Phys. Rev. B **31**, 4403 (1985); S. White, D. Scalapino, R. Sugar, E. Loh, J. Gubernatis, and R. Scalettar, *ibid.* **40**, 506 (1989).

[5] Z. W. Salsburg, J. D. Jacobson, W. Fickett, and W. W. Wood, J. Chem. Phys. **30**, 65 (1959).

[6] J. Valleau and D. Card, J. Chem. Phys. **57**, 5457 (1972).

[7] A. Ferrenberg and R. Swendsen, Phys. Rev. Lett. **61**, 2635 (1988); **63**, 1658(E) (1989); R. Swendsen, Comput. Phys. Commun. **65**, 281 (1991); R. Swendsen, Physica A **194**, 53 (1993); A. Ferrenberg, D. Landau, and R. Swendsen, Phys. Rev. E **51**, 5092 (1995).

[8] J. Hirsch, Phys. Rev. B **28**, 4059 (1983).

[9] For values of $U/t \gtrsim 12$, Scalettar *et al.*, [Phys. Rev. B **44**, 10 502 (1991)] found that determinant QMC calculations, such as the ones being performed here, fail to explore the phase-space ergodicly and the simulations become trapped at single values of the density, n. The simulations described here for $U/t = 8$, clearly sample (see Fig. 1) multiple values of n, and do not have this problem.

[10] B. Efron and G. Gong, Am. Stat. **37**, 36 (1983).

[11] M. E. J. Newman and R. G. Palmer, cond-mat/9804306 (unpublished).

[12] E. Loh, Jr., J. Gubernatis, R. Scalettar, S. White, D. Scalapino, and R. Sugar, Phys. Rev. B **41**, 9301 (1990).

[13] J. Hirsch and S. Tang, Phys. Rev. Lett. **62**, 591 (1989).

[14] C. Au and B.-H. Zhao, cond-mat/9602054 (unpublished); M. Simon and A. Aligia, Phys. Rev. B **53**, 15 327 (1996); G. Su, *ibid.* **54**, 8281 (1996); E. Ercolessi, P. Pieri, and M. Roncaglia, Phys. Lett. A **233**, 451 (1997); C. Hellberg and E. Manousakis, Phys. Rev. Lett. **78**, 4609 (1997); M. Kohno, Phys. Rev. B **55**, 1435 (1997); A. C. Cosentini, M. Capone, L. Guidoni, and G. B. Bachelet, cond-mat/9801299 (unpublished).